

# Elucidation of Phosphoproteins Involved in the Renal Cellular Response to Acute Metabolic Acidosis

BY EMI OKAYASU WITH DANA M. FREUND,  
JESSICA E. PRENNI, AND NORMAN P. CURTHOYS  
CALVIN COLLEGE, GRAND RAPIDS, MI WITH CSU DEPARTMENT OF BIOCHEMISTRY

## Abstract

Metabolic acidosis is caused by a decrease in plasma pH and the concentration of bicarbonate buffer in the blood. The proximal tubule cells of the kidney mediate the body's response to this pH stress by increasing the catabolism of glutamine, effectively producing bicarbonate for export to the bloodstream.<sup>[1]</sup> Though this response is well characterized, the mechanisms by which this response is activated are unknown.<sup>[2]</sup> In order to investigate the various pathways which might be involved in initiating this response, a proteomic analysis of the phosphoproteins expressed by proximal tubule cells modeling metabolic acidosis was done. The phosphoproteins expressed by these cells after a 24 hour treatment at pH 6.9 were run on 2D gels, and stained with a quantitative phosphoprotein stain and total protein stain. Analysis was performed with imaging software, and finally proteins were identified by LC-MS/MS and studied for their functional characteristics. Using this approach, both phosphoproteins abundant in the proteome of proximal tubule cells as well as many proteins changing in degree of phosphorylation were found.

## Introduction

Metabolic acidosis is a condition characterized by a decrease in blood pH due to the overproduction of acid or a decrease in bicarbonate recovery by the kidney. Under

normal physiological conditions, the bicarbonate ions act as a buffer, maintaining an equilibrium blood pH level of approximately 7.4. During metabolic acidosis, the higher concentrations of acid in the blood and decreased recovery of bicarbonate stimulate a pH response in the proximal tubule cells of the kidney.<sup>[2]</sup> This cellular response restores blood pH by increasing renal uptake and catabolism of glutamine (Figure 1). Once in the cell, glutamine is transported into the mitochondria and converted into the citric acid cycle intermediate  $\alpha$ -ketoglutarate by the enzymes glutaminase (GA) and glutamate dehydrogenase (GDH). Intermediates of the citric acid cycle are exported to the cytoplasm, where the cytosolic phosphoenolpyruvate carboxykinase (PEPCK) converts oxaloacetate to phosphoenolpyruvate. Stimulation of the citric acid cycle and the en-

zymatic activity of PEPCK produce bicarbonate ions.<sup>[2]</sup> Two key transporters which are up-regulated in this response are the luminal  $\text{Na}^+/\text{H}^+$  antiporter (NHE3), which acidifies the urine bound for excretion, and the basolateral  $\text{Na}^+/\text{HCO}_3^-$  symporter (NBC1), which releases the bicarbonate ions into the bloodstream to increase the pH.<sup>[3]</sup>

Although this pH-sensitive cellular response has been well characterized, the signaling pathways which stimulate this response remain unknown. The possible pathways remain difficult to elucidate because of complex regulatory interactions between mRNA and the proteins they encode. While some of the key enzymes are up-regulated during the response by increased levels of transcription, other enzymes are regulated by increased stabilization of their respective mRNA transcripts.<sup>[4]</sup>

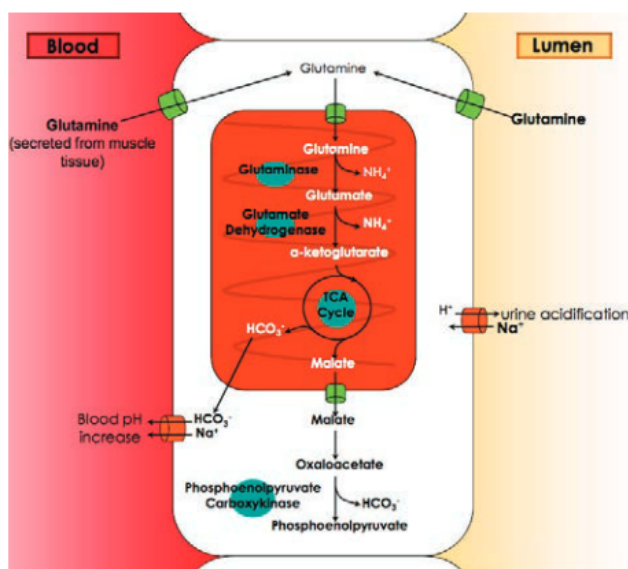


**Figure 1:** Response Mechanism for Increased Catabolism of Glutamine by the Proximal Tubule Cell During Metabolic Acidosis. Glutamine is imported into the cell and reduced in the mitochondria to the citric acid cycle intermediate,  $\alpha$ -ketoglutarate, which is then converted to malate by the enzymes of the citric acid cycle. Malate is converted to phosphoenolpyruvate in the cytoplasm. The 2  $\text{HCO}_3^-$  ions produced in this process are exported to the bloodstream, while  $\text{H}^+$  enter the lumen of the kidney bound for excretion in the urine.

This characterization of the proteome of renal proximal tubule cells focuses on protein regulation and post-translational modifications. As phosphorylation is one of the most important post-translational modifications in the regulation of proteins, this project will focus on the differences in the phosphoproteomes between control cells (grown in pH 7.4 media) and cells modeling metabolic acidosis (pH 6.9 media, 24 h treatment). Identification of phosphoproteins that are present during metabolic acidosis will elucidate how the adaptive response is mediated by proximal tubule cells. Characterization of expression changes that occur specifically in the phosphoprotein fraction will enable a more targeted investigation of how the signals are mediated specifically at the protein level.

## Materials and Methods

**Mammalian cell culture:** Wistar-Kyoto rat proximal tubule (WKPT) cells were grown from stocks stored at  $-80^{\circ}\text{C}$ . The WKPT cell line was used because the rat genome has been sequenced, and comprehensive knowledge of the genome is necessary for subsequent identification by mass spectrometry. Cells were plated and grown in a  $37^{\circ}\text{C}$  incubator with pH 7.4 media to confluence. Once confluent, the cells were split onto seven new plates. 24 h before harvesting the proteins for phosphoprotein fractionation, three plates were treated with pH 6.9 media and three plates were incubated with pH 7.4 media to model acute metabolic acidosis. 12 h before harvesting, the media was replenished in order to ensure that any changes observed were due to the pH treatment rather than stress due to starvation.<sup>[5]</sup>

## Phosphoprotein Fractionation

24 h treated cells were lysed and

proteins were purified with CHAPS detergent, nucleases, and protease inhibitors. The whole cell lysate from the three control (pH 7.4 media) plates was pooled and approximately 2.5 mg of protein was applied to a QIAGEN phosphoprotein purification column, which binds the phosphate groups of phosphorylated amino acid residues. This process was repeated for the plates treated with pH 6.9 media. The non-phosphoprotein flow through was collected and analyzed on a western blot to ensure that the non-phosphorylated fraction did not contain a significant amount of phosphorylated protein. The columns were washed, and phosphoproteins were eluted with a phosphate buffer. Halt phosphatase inhibitor cocktail was added to the fractions as they were collected.<sup>[5]</sup> Four sets of phosphoprotein columns were run in order to obtain enough phosphoprotein for three technical replicates of 6.9 and 7.4 2D gels.

**Bradford Assays:** Bradford assays were performed both before and after phosphoprotein fractionation to quantify the amount of protein initially being applied to the column and to calculate the yield of phosphorylated protein collected from the column. A standard curve was generated using known concentrations (0.5, 1.0, 2.0, 5.0, 7.5, 10.0 mg/ml) of BSA. Absorbance was measured on a Beckman DU 640 UV/Vis Spectrophotometer at 595 nm.<sup>[6]</sup> The protein samples collected during fractionation were concentrated on NanoSep ultrafiltration columns (MWCO 10 kDa), and the final concentration of phosphoprotein was interpolated using the standard curve generated on the spectrophotometer.

**2-Dimensional (2D) Gel Electrophoresis and Protein Staining:** The concentrated fractions of phosphoprotein were precipitated and salts removed with a Bio-rad Ready Prep

2D clean-up kit. The protein was then dissolved in rehydration buffer and used to rehydrate an immobilized pH gradient (IPG) gel strip (11 cm, pH range 3-6) for isoelectric focusing. Phosphorylation is a post-translational modification that lowers the isoelectric point (pI) of a protein, thus IPG gel strips with a narrow pH range of 3-6 were used to allow for optimal resolution of phosphoprotein spots. Each IPG strip for the isoelectric focusing was rehydrated with 100  $\mu\text{g}$  of phosphoprotein. Pre-cast SDS-PAGE gels (8x11 cm) loaded with 2  $\mu\text{l}$  Peppermint stick protein marker containing both phosphorylated and non-phosphorylated protein standards were used for separation along the second dimension. For imaging, the gels were first stained with ProQ Diamond phosphoprotein fluorescent gel stain (Invitrogen) which only binds phosphate groups, enabling quantification of phosphoproteins by comparison of spot volume intensities. In addition to staining with Pro-Q Diamond Phosphoprotein Gel Stain, the gels were also stained with SYPRO Ruby Protein Gel Stain (Invitrogen), which non-covalently interacts with the peptide backbone of all proteins<sup>[5]</sup>.

**Image Analysis:** Gel images were analyzed using Delta 2D software to align gel spots, both between technical replicates and between pH 6.9 and pH 7.4 conditions. Spots that exhibited significant changes in intensity between the conditions were excised from gels with a Genomic Propic II robot for identification by mass spectrometry.

## Protein identification

Protein spots of interest were digested using the ProteaseMax (Promega) in-gel tryptic digest procedure, which includes reduction of disulfide bonds with dithiothreitol (DTT), alkylation with iodoacetamide (IAA), and 3 h tryptic diges-

tion in ProteaseMax surfactant. 2  $\mu$ l of the peptide mixture for each sample was analyzed by LC-MS/MS (Thermo Scientific LTQ linear ion trap) using a 42 min linear gradient from 25%-55% buffer B (90% ACN, 0.1% formic acid) ACN gradient. MS2 scans were collected for all samples and MS3 scans were triggered upon detection of a neutral loss of phosphoric acid.

Bioinformatics: MS2 spectra were searched against the Rat protein sequence database (maintained by the International Protein Index) using the Mascot and Sorcerer/Sequest database search engines. The protein identifications were compiled into Scaffold software (Proteome Software), which was used to manually confirm and validate the protein identifications. Identified proteins were investigated on the online databases [www.uniprot.org](http://www.uniprot.org) and [www.phosphosite.org](http://www.phosphosite.org) to determine biological function.

## Results

### Protein Fractionation and Separation

Gels were imaged both after the application of the phospho-specific ProQ Diamond stain and after total protein staining with Sypro Ruby (Figure 2). In total, six 2D gels were run (6.9 and 7.4 in triplicate) and 12 images were collected. However, only the first set of gels was used for image analysis and subsequent protein spot identification due to poor resolution of spots in the second and third sets.

### Western Blot Verification of Phosphoprotein Fractionation

Verification of the purity of the phosphoprotein fraction eluted from the column was carried out by western blotting. The non-phosphoprotein fractions collected from both the pH 6.9 column and the pH

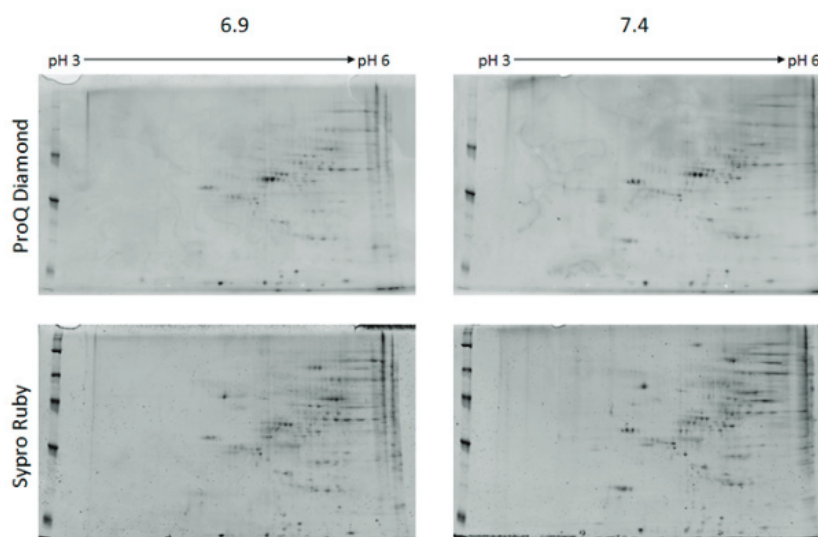


**Figure 2:** Comparison of 2-Dimensional Gel Images. Gels were stained with the phosphoprotein stain ProQ Diamond, then re-stained and re-imaged with the total protein stain Sypro Ruby. The peppermint stick molecular weight marker (on the left of each gel) contains two phosphoproteins, which are visible in the ProQ stained gels. All six bands of the marker are visible in the Sypro-stained gels.

7.4 column were concentrated on a 10 kDa MWCO spin column and run on a gel alongside phosphoprotein fractions leftover after rehydration of the IPG strip. The resulting gel was transferred to a polyvinylidene fluoride membrane and blotted with an antibody for the known abundant phosphoprotein p44/42 MAPK (44 and 42 kDa) as well as an antibody for the non-phosphoprotein GAPDH (36 kDa). Figure 3 shows that the phosphoprotein fractionations were successful in purifying the phosphoproteins from

the non-phosphoproteins. Though there is a small amount of non-phosphoprotein in the phosphoprotein sample, this blot shows that there is no loss of phosphoprotein in the flow-through during fractionation. Relative intensity of the probes was not quantified as different amounts of protein were loaded into each lane.

### Delta 2D Quantitation Analysis

Of the 3 gel sets that were run,

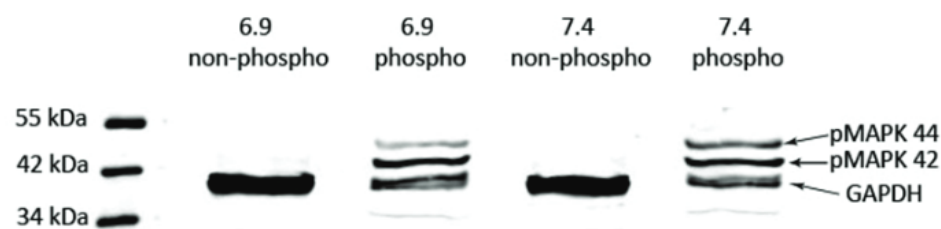


**Figure 3:** Western Blot of Fractions Collected from the Phosphoprotein Columns. Probing with the antibody for phospho-p44/42 MAPK, it is apparent that the second and fourth lanes with the phosphoprotein fractions from 6.9 and 7.4 contain mainly phosphoprotein. GAPDH is found mostly in the first and third lanes, which contain the non-phosphoprotein fractions from 6.9 and 7.4, respectively.

Spot	Protein	Change in expression in 6.9	Fold change	Function
1	Hsc70-interacting protein Nuclear Ribonuclear Protein Protein Disulfide Isomerase A6	↑Phosphorylation	1.90	ER Chaperone mRNA Processing Protein Folding
2	Hepatoma Derived Growth Factor	↑Phosphorylation	1.66	Nephrogenesis
3	Transcription elongation factor Astrocytic Phosphoprotein	↑Phosphorylation	1.68	Protein Synthesis Anti-apoptosis
4	60S acidic ribosomal protein*	↑Phosphorylation	1.57	Protein Synthesis
5,6	78 kDa GRP*	↓Phosphorylation	0.44, 0.49	ER Chaperone
7	Transcriptional activator Calponin-3	↑ total protein abundance	1.81	Nucleotide Binding Cytoskeletal Organization
8,9	Tropomyosin*	↓ total protein abundance	0.62, 0.63	Cytoskeletal Organization
10	Proteasome subunit alpha	↓ total protein abundance	0.48	Protein Degradation
11	Endoplasmic*	↓ total protein abundance	0.31	ER Chaperone
12	Naca Protein	↓ total protein abundance	0.60	Subcellular Protein Localization

**Table 1:** Phosphoproteins Changing during the Response to Metabolic Acidosis. Changes in phosphorylation were calculated based on the ratio of spot intensity in the ProQ-Diamond stained gels from pH 7.4 to pH 6.9. Changes in total protein abundance were calculated based on the ratio of spot intensity in Sypro stained gels from 7.4 to 6.9. Proteins denoted with \* have been previously identified as changing during a 24 h response to metabolic acidosis.<sup>[5]</sup>

only the first set of gels was used for analysis and quantification due to insufficient resolution and problems with the IEF in the second and third sets. Spot intensity ratios were determined by Delta 2D based on the volume of corresponding gel spots. The spot intensity ratio of the 6.9 gel to the 7.4 gel was calculated individually for all spots on both the SYPRO stained image and the ProQ Diamond stained image. Comparison of the change in total phosphoprotein (6.9 Sypro/7.4 Sypro) to the change in phosphorylation state of the protein (6.9 ProQ Diamond/7.4 ProQ Diamond) indicated whether the observed spot change was due to a change in total protein abundance or a change in phosphorylation. By comparing these two ratios, 12 protein spots were found to be significantly changing (Table 1). Only one set of gel images was used to calculate quantitative changes in protein expression. Thus, in order to be counted as significantly changing, only spots that showed

a fold change of magnitude greater than 1.5 were considered.

### Protein Identification by LC-MS/MS

In total, 30 spots were picked from each gel and pooled with the corresponding spot before undergoing tryptic digestion. From these 30 pairs of matching spots, 34 proteins were identified (Table 2). In addition to identification of proteins from each of the 30 protein spots, in one of these spots, a phosphorylation site was detected by neutral loss scanning. A neutral loss peak was detected in the MS2 scan, indicating a loss of phosphoric acid (H<sub>3</sub>PO<sub>4</sub>) from a serine residue on the phosphopeptide (Figure 4a).

Protein	Unique peptides	Function
Astrocytic phosphoprotein	3	Anti-apoptotic Protein
Catechol O-methyltransferase	3	Cell Signaling
Similar to Chromobox protein	2	Chromatin Rearrangement
Tropomyosin	14,21,17	Cytoskeletal Organization
Calponin-3	5,6,7	Cytoskeletal Organization
WAS protein family, member 2	4	Cytoskeletal Organization
Na(+)/H(+) exchange regulatory cofactor	2	Cytoskeletal Organization
NSFL1 cofactor p47	14,14	Golgi Organization
RNA-binding protein	3	mRNA processing
Nuclear ribonucleoprotein F	2,2	mRNA processing
Hepatoma-derived growth factor	3,3,3,3	Nephrogenesis
Transcriptional activator protein Pur-beta	11,9,5	Nucleotide Binding
Proteasome subunit alpha	3	Protein Degradation
Thioredoxin-like protein	2	Protein Degradation
78 kDa GRP	32, 35, 2	Protein Folding in ER
Calreticulin	15	Protein Folding in ER
Endoplasmic	20	Protein Folding in ER
Hsc70-interacting protein	4,6	Protein Folding in ER
Protein disulfide-isomerase A4	4	Protein Folding in ER
Tetratricopeptide repeat-containing protein	4	Protein Folding in ER
Protein disulfide-isomerase A6	2	Protein Folding in ER
Hsp90 co-chaperone Cdc37	2	Protein Folding in ER
Elongation factor 1-delta	10,11	Protein Synthesis
Nucleophosmin	3,2,3	Protein Synthesis
60S acidic ribosomal protein	6	Protein Synthesis
Transcription elongation factor B	3	Protein Synthesis
Cortactin	7,8	Receptor Mediated Endocytosis
Naca Protein	8	Subcellular Protein Localization
Chromobox homolog 3	3,3	Transcriptional Regulation
Small ubiquitin-related modifier	2	Transcriptional Regulation
Similar to chromobox homolog 3	2	Transcriptional Regulation

**Table 2:** Proteins Identified by LC-MS/MS. 30 spots were excised from the gels, digested with trypsin, and identified by LC-MS/MS analysis. The number of unique peptides indicates how many of the peptides unique to a given protein were found and used to match the peptide to the protein.

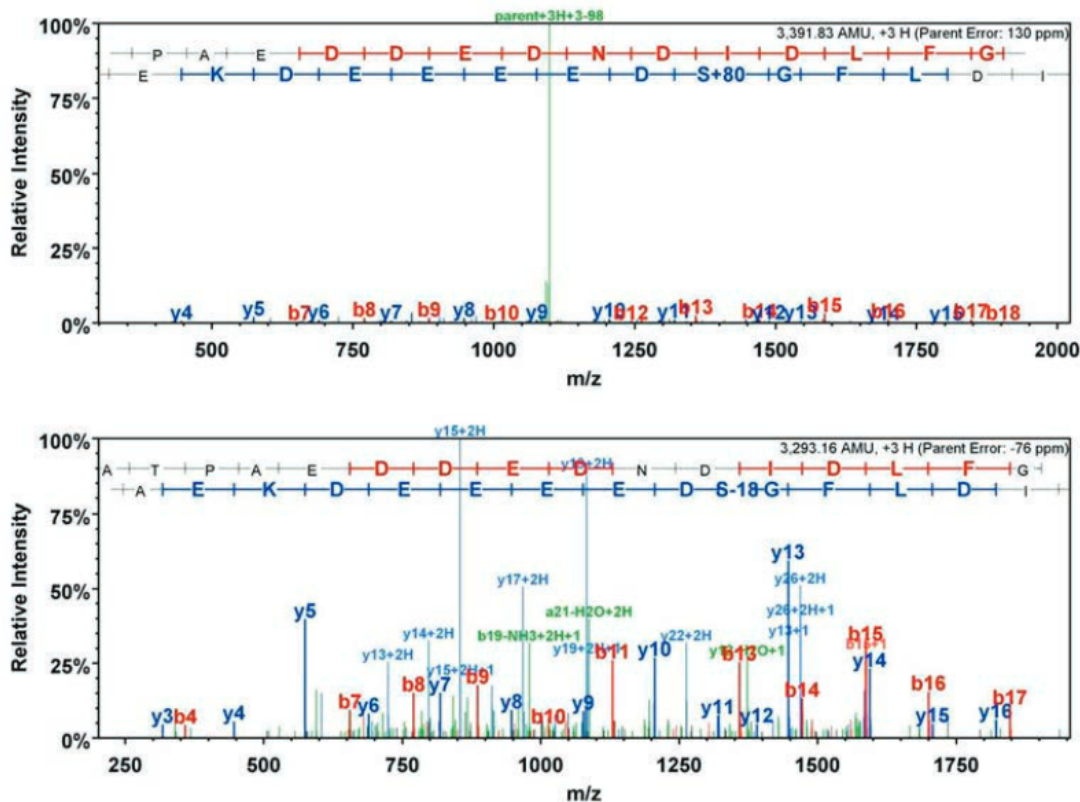


Figure 4: Identification of Phosphorylation site by Neutral Loss Scanning. 4A shows the MS2 scan of a phosphopeptide. The neutral loss of phosphoric acid causes decreased fragmentation along the peptide backbone, as seen by the low relative intensity of the b and y ions. During the neutral loss scanning method, the de-phosphorylated peptide is selected and fragmented in a third MS3 scan (4B). This spectrum shows greater fragmentation along the peptide backbone, as indicated by the higher intensity of the b and y ions. This enables greater confidence in peptide identification as well as identification of the exact residue of phosphorylation.

When intense enough, this neutral loss peak triggers a third MS3 scan in which the peptide is further fragmented in order to obtain a spectrum from which the primary sequence of amino acid residues can be confirmed and the specific phosphorylated residue identified. One phosphorylation site was confirmed by the subsequent MS3 scan. Phosphorylation of S531 on Isoform 2 of Elongation factor 1-delta was detected by the neutral loss peak in the MS2 scan and confirmed by the improved fragmentation in the MS3 scan (Figure 4b).

## Discussion

A complete characterization of the proteomic response to metabolic acidosis would require a more comprehensive and replicable data set than provided by the scope of this

investigation. The proteins identified as changing during metabolic acidosis in this experiment confirm and support previous findings.<sup>[5]</sup> Of the 12 proteins identified as changing from pH 7.4 to pH 6.9, five were previously identified as changing in either phosphorylation or total abundance in a prior 2D gel analysis of WKPT cells during 24 h metabolic acidosis.<sup>[5]</sup> These common proteins are denoted by an asterisk in Table 1. Also, many of the proteins identified in this study have been shown to interact with the proteins found to be changing in this prior study.<sup>[5]</sup> Most notably, the cytoskeletal protein actin, which previously showed a 2.1 fold increase in phosphorylation, is known to interact with three of the proteins identified in this study: cortactin isoform C, Na<sup>+</sup>/H<sup>+</sup>-exchange regulatory cofactor NHE RF-1, and Isoform 1 of troppomyo-

sin alpha-3 chain. Another protein that was previously found to be increasing in phosphorylation is the stress response chaperone protein, Heat shock cognate 71 (also denoted Hsc 70). Though Hsc 70 itself was not identified in any of the spots analyzed in this study, Hsc 70 interacting protein was found in one of the spots. Hsc 70 interacting protein stabilizes Hsc 70 in its ADP-bound state, thereby increasing its affinity for substrate proteins that require the chaperone activity of Hsc 70 in order to fold correctly. An additional 7 proteins associated with protein folding in the ER were also identified, four of which were found previously to be changing in either phosphorylation or total abundance during metabolic acidosis.

The prevalence of ER luminal chaperone and folding proteins could be a result of the changes in

the proteome that the cell must undergo in response to the change in pH. In order to restore acid-base balance in the blood, the proximal tubule cell must increase the catabolism of glutamine, which requires increased expression of the enzymes involved in this pathway. Thus, chaperone proteins are essential in mediating the adaptive response. The various functions of these proteins related to protein folding in the ER include co-chaperones that maintain activity of Hsp70 and Hsc70, disulfide isomerases which are essential to stabilizing the tertiary and quaternary structures of mature proteins, and quality control proteins that are associated with degradation of misfolded proteins found in the ER.

Though there appears to be a prevalence of proteins associated with folding and chaperone activity among the various proteins identified in this study, it is difficult to quantify statistically significant changes in the proteome with a limited number of replicates and the low reproducibility rate of 2D gel data in this study. However, the preliminary results of this study do correlate with findings from previous studies. Thus, potential future directions for characterizing the response of proximal tubule cells to metabolic acidosis include running more replicates of 2D gels in order to gain statistical p-values for fold changes based on spot intensity between the two gels. Finally, one aspect of this study that was not fully exploited was the use of neutral-loss scanning on the LC-MS/MS to detect specific amino acid residues that were phosphorylated. The neutral loss of phosphoric acid triggered an MS3 scan for a small minority of samples that were run, and only one phosphosite was definitively identified using this technique. By enriching for phosphopeptides before scanning, however, it may be possible to confirm phosphosites on

a greater number of peptides, and even detect novel phosphosites on previously uncharacterized phosphoproteins.

### Acknowledgements

We acknowledge support from the Proteomics and Metabolomics Facility. We also thank Lynn Taylor and Dr. Mam Scherman. This work was supported by the Summer Program in Molecular Biosciences Research Experience for Undergraduates funded by the National Science Foundation.

### References

- [1] Horie S, Moe O, Tejedor A, Alpern R J. Preincubation in acid medium increases Na/H antiporter activity in cultured renal proximal tubule cells. *Proc Natl Acad Sci* 87 (12): 4742-5, 1990
- [2] Curthoys N P. Role of Mitochondrial Glutaminase in Rat Renal Glutaminase Metabolism. *J Nutr* 2491-2495, 2001.
- [3] Olson BJ, Markwell J: Assays for determination of protein concentration. *Curr Protoc Protein Sci Unit 3: Chapter 3*, May 2007
- [4] Curthoys N P, Taylor L, Hoffert J D, Knepper M A. Proteomic analysis of the adaptive response of rat renal proximal tubules to metabolic acidosis. *Am J Physiol Renal Physiol* 292: F140-147, 2007.
- [5] Gammelgaard, D. Preliminary Proposal, Spring 2010. Colorado State University Department of Biochemistry.
- [6] Taylor L, Curthoys N P. Glutamine metabolism: role in acid-base balance. *Biochem Molec Biol Ed* 32: 291-304, 2004.